01

Heat transfer in wide-aperture absorbing loads of liquid microwave calorimeters

© A.I. Klimov, V.Yu. Konev

Institute of High Current Electronics, Siberian Branch, Russian Academy of Sciences,
634055 Tomsk, Russia
e-mail: klimov@lfe.hcei.tsc.ru

Received June 17, 2024
Revised August 29, 2024
Accepted October 1, 2024

Using the CST Microwave Studio program, thermal processes were simulated in wide-aperture disk-shaped absorbing loads of calorimeters with a working fluid based on ethyl alcohol while absorbing the energy of high-power microwave pulses. The loads with flat and ribbed input windows at carrier frequencies 3 and 10 GHz were investigated. We analyzed the features and optimal conditions for using the CST Microwave Studio package in relation to the tasks being solved. For flat input windows, simulation results are compared with analytical estimates based on the problem of cooling a half-space filled with a homogeneous medium having a temperature jump at the initial moment of time. Time dependences of heat leakage from working fluid into the input windows were obtained during time interval of the high-power microwave pulses energy measurement with the calorimeter. The underestimation of the measured energy relative to the microwave energy released in the working fluid was calculated.

Keywords: high-power microwave pulses, thermal processes, working fluid, ribbed dielectric input window, numerical simulation, CST Microwave Studio

DOI: 10.61011/TP.2024.11.59741.205-24

Introduction

Liquid calorimeters [1] with disc-shaped wide-aperture absorbing loads are successfully used to measure the energy of high-power microwave pulses. The operation of calorimeters is based on measuring the increase in the volume of an ethyl alcohol-based working fluid filling the load when absorbing the energy of a microwave pulse. Calorimeters with manual and electronic control have been developed to date. The measurement time of the absorbed energy is several seconds. It is close to the time of the mechanical reaction of the calorimeter load.

Figure 1 shows a schematic drawing and the appearance of a disk-shaped absorbing load with a ribbed input window. The load housing is made of high-density polyethylene, and the shape of the load, including the geometry of the ribbed input window, was optimized by computer simulation for achieving a minimum reflectance of microwaves.

The absorption of the energy of microwave pulses in the working fluid is accompanied by the emergence and development of thermal processes, which manifest themselves in the leakage of part of the heat into the dielectric input window of the absorbing load and, consequently, an underestimation of the measured energy. The first attempt to study these processes in relation to wide-aperture absorbing loads with flat input windows using the CST Microwave Studio software package in comparison with analytical estimates was made in Ref. [2]. However, the subsequent analysis of the results of this work showed the need for a more detailed study and clarification of the conditions of use of the CST Microwave Studio software package, and in relation not only to absorbing loads with flat, but also, more importantly, with ribbed input windows, which is the subject of this study.

1. Analytical estimates for a wide-aperture absorbing load model with a flat input window

First of all, the analysis of a simpler case of a wide-aperture disk-shaped absorbing load with a flat input

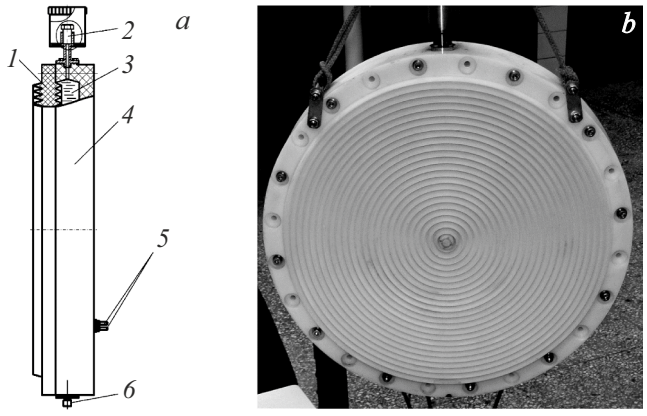

Figure 1. Schematic drawing (*a*) and appearance (*b*) of a three-centimeter band calorimeter disk-shaped wide-aperture absorbing load from the side of the input window [1]: *1* — ribbed input window; *2* — filler plug; *3* — working fluid; *4* — lid; *5* —contacts of heating coils; *6* —drain plug.

window is of interest (Fig. 2). Such a load can also be used in a liquid microwave calorimeter [3].

Ethyl alcohol is a medium that strongly absorbs microwave radiation, for this reason the microwave energy is released near the interface between the working fluid and the dielectric. In the case of a ribbed window, the energy release is also concentrated near the dielectric, and heat transfer processes may have common features with heat transfer processes in the case of a flat window. The flat geometry of the load makes it possible to make analytical estimates, the results of which are of interest for comparison with the results of computer simulation.

A rigorous analytical consideration of the heat transfer process, even in the case of flat geometry, is a challenging task. An analysis based on the results of solving the well-known problem [4] of cooling of a half-space (Fig. 3) filled with a homogeneous medium having a temperature jump at the initial moment of time can provide some clarity.

The use of a solution to this problem in the first approximation seems justified since the thermodynamic characteristics of polyethylene and ethyl alcohol do not differ very much.

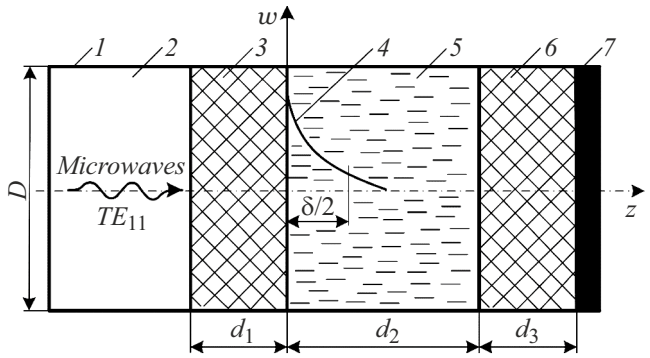

Figure 2. Calculated geometry of a disk-shaped absorbing load with a flat input window with a diameter much larger than the wavelength, $D \gg \lambda$: *1* — waveguide; *2* — air; *3* — flat polyethylene input window; *4* — density distribution of absorbed microwave energy; *5* — alcohol; *6* — back polyethylene wall; *7* — microwave absorber.

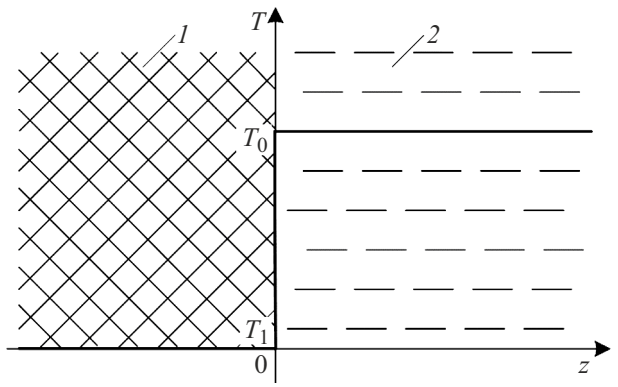

Figure 3. For problem of the half-space cooling: *1* — polyethylene; *2* — alcohol.

The ambient temperature $T = T_0$ is everywhere at the initial time $t = 0$ at $z > 0$. The temperature T_1 of the surface $z = 0$ is always constant, $T_1 < T_0$. It is necessary to find the temperature distribution of the medium $T(z, t)$ in the half-space $z > 0$ for the time points $t \geq 0$. The medium to the right of the plane $z = 0$ simulates ethyl alcohol in an absorbing load and has the corresponding physical characteristics. The plane $z = 0$ itself corresponds to the interface between the alcohol and the dielectric of the input window. The temperature distribution $T(z, t)$ is described by the thermal conductivity equation [4]:

$$\frac{\partial T}{\partial t} = \chi \frac{\partial^2 T}{\partial z^2}, \qquad \chi = \frac{\kappa}{\rho c_v},$$

where χ — thermal diffusivity coefficient, κ — coefficient of thermal conductivity, ρ and c_v — density and specific heat of alcohol at constant volume, respectively.

The solution of the problem for $t \geq 0$ has the form

$$T(z, t) = 2\frac{T_0 - T_1}{\sqrt{\pi}} \int_0^{\frac{z}{2\sqrt{\chi t}}} \exp(-\xi^2) d\xi + T_1,$$

$$\frac{\partial T(z, t)}{\partial z} = \frac{T_0 - T_1}{\sqrt{\pi \chi t}} \exp\left(-\frac{z^2}{4\chi t}\right),$$

$$\frac{\partial T(0, t)}{\partial z} = \frac{T_0 - T_1}{\sqrt{\pi \chi t}},$$

therefore, it is possible to estimate the dependence of the thermal power density $p_0(t)$ and the heat flux density $\Delta w_0(t)$ on time across the interface between liquid and dielectric $z = 0$:

$$p_0(t) = \kappa \frac{\partial T(0, t)}{\partial z} = \kappa \frac{T_0 - T_1}{\sqrt{\pi \chi t}},$$

$$\Delta w_0(t) = \int_0^t p_0(t') dt' = 2\kappa (T_0 - T_1) \sqrt{\frac{t}{\pi \chi}}. \qquad (1)$$

The following values of the characteristics of ethyl alcohol [5–7] were used for the temperature 20°C in the following estimates: $\rho = 789\,\text{kg/m}^3$, $c_v = 2130\,\text{J/(kg·K)}$, $\kappa = 0.1705\,\text{W/(m·K)}$, $\chi = 0.904169 \cdot 10^{-7}\,\text{m}^2/\text{s}$, and $c_p = 2390\,\text{J/(kg·K)}$ — specific heat capacity of alcohol at constant pressure.

The temperature increment $\Delta T = (T_0 - T_1)$ required to calculate the dependencies $p_0(t)$ and $\Delta w_0(t)$ was estimated for frequencies $f = 3$ and 10 GHz on the symmetry axis of the circular waveguide for the wave TE_{11} with a vertically directed electric field falling from the air onto a layered structure (Fig. 2). A microwave pulse with a rectangular envelope and a power amplitude of $P = 580\,\text{MW}$ at a duration of $\tau = 100\,\text{ns}$ (energy 58 J) was set in analytical estimates and computer simulation. The polyethylene thickness d_1 for both loads with a flat input window was optimized during the numerical simulation described below

Table 1. Calculated parameters of the absorbing load model with a flat input window

f, GHz	λ, mm	D, mm	d_1, mm	d_2, mm	d_3 mm	K, dB	T_{tr}, MW	W_{tr}, J
3	100	600	17.5	45	25	−10.26	525	52.5
10	30	200	5.8	45	25	−12.3	546	54.6

for minimizing the reflectance of microwaves K_r and the power P_{tr} and energy $W_{tr} = P_{tr}\tau$ transmitted to alcohol were calculated taking into account this reflectance. The alcohol thickness d_2 was sufficient to almost completely absorption the energy of the microwave pulse, so that the reflection from the rear polyethylene wall with a thickness of d_3 can be neglected. The computer simulation showed that changes of conditions on the outside of the rear wall, namely the installation of a reflective metal plate or the presence of an air layer between the wall and an ideal microwave absorber in both the model with a flat input window and the models described below with ribbed input windows, did not significantly affect the calculation results. The parameters for calculations in the case of a model with a flat input window are listed in Table 1.

The dispersion of the waveguide can be neglected since the condition $D \gg \lambda$ is fulfilled for both frequencies, and it is possible to use the expression for the electric field of a plane wave propagating in a medium with absorption [8]: $E(z,t) = E_0 \exp[(j(\omega t - kz))]$, where E_0 — the amplitude of the electric field of the wave, $\omega = 2\pi f = 2\pi c/\lambda$ — angular frequency, c — the speed of light in vacuum. Since the alcohol is a medium with losses, the wave number is complex: $k = k' + jk''$, where

$$k'k'' = \pm\frac{2\pi f}{c}\sqrt{0.5\left[\sqrt{\varepsilon'^2(f) + \varepsilon''^2(f)} \pm \varepsilon'(f)\right]}.$$

Here $\varepsilon'(f)$ and $\varepsilon''(f)$ are the real and imaginary parts of the dielectric constant of alcohol, respectively. Thus, the electric field of the wave in alcohol is attenuated in accordance with the ratio: $E(z,t) = E_0 \exp[j(\omega t - k'z)]\exp(k''z)$. The value $\delta = 1/|k''|$ is the spatial scale of the field attenuation. Since the density of the wave power flux $\sim |E(z,t)|^2$, the spatial scale of the decrease of the density of absorbed power and the density of absorbed energy is equal to $\delta/[2 = 1/(2|k''|)$, i.e. two times less than the spatial scale of field attenuation, and $p_{tr}(z) = p_{tr0}\exp(-2z/\delta)$ — the density of the microwave power flux near the dielectric−alcohol interface.

Calculations were performed using $\varepsilon'(f)$ and $\varepsilon''(f)$ obtained by approximating, according to the Debye formula, respectively, the real and imaginary parts of the dielectric constant of 95% ethyl alcohol based on the data of Ref. [9]. For $f = 3\,\text{GHz}$ $\varepsilon'(f) = 10.1$, $\varepsilon''(f) = 9.4$. For $f = 10\,\text{GHz}$ $\varepsilon'(f) = 6.0$, $\varepsilon''(f) = 3.4$. For polyethylene $\varepsilon'(f) = 2.25$, $\varepsilon''(f)/\varepsilon'(f) = 0.0004{-}0.0005$ [10], and the absorption of microwave energy in the input window can be neglected.

The power ΔP_{tr} released in a thin layer $\Delta z \ll \delta/2$ of the working fluid within a small circle with an area of S near the waveguide axis (Fig. 2):

$$\Delta P_{tr} = S[p_{tr}(z) - p_{tr}(z+\Delta z)] = p_{tr0}S\{\exp(-2z/\delta) -$$

$$- \exp[-2(z+\Delta z)/\delta]\} \approx p_{tr0}S(2\Delta z/\delta)\exp(-2z/\delta).$$

$z = 0$ near the window and $\Delta P_{tr} = 2p_{tr0}S\Delta z/\delta = 2p_{tr0}V/\delta$, where $V = S\Delta z$ is the volume of the layer. The energy released in the layer:

$$\Delta P_{tr}\tau = 2p_{tr0}\tau V/\delta = mc_p(T_0 - T_1) = \rho V c_p(T_0 - T_1),$$

where $m = \rho V$ — the mass of the alcohol layer, and the temperature difference

$$\Delta T = T_0 - T_1 = 2p_{tr0}\tau/(\delta\rho c_p). \quad (2)$$

The densities of the power flux p_{tr0} and the energy flux $w_{tr0} = p_{tr0}\tau$ were estimated using a formula linking the microwave power P_{tr} transmitted to alcohol and the electric field strength E of wave TE_{11} on the axis of the circular waveguide [11]. In the case of $D \gg \lambda$, $E^2_{\text{kV/cm}} = 6320P_{tr\text{MW}}/(\pi D^2_{\text{cm}})$. At the same time, the wave front shape is close to the plane shape near the waveguide axis, so it is possible to use a formula linking the field strength and the power flux density for a plane wave: $E^2_{\text{kV/cm}} = 729p_{tr0\text{MW/cm}^2}$, from where $p_{tr0\text{MW/cm}^2} = 8.67P_{tr\text{MW}}/(\pi D^2_{\text{cm}})$. The results of calculations of temperature increments ΔT using the formula (2) are listed in Table 2. The dependences on the time of relative heat dissipation $\Delta w_0/w_{tr0}$ from the working fluid to the dielectric were calculated using the obtained temperature increments and the ratio (1). They are shown below in Fig. 4.

Table 2. Results of calculations of the temperature increment at the alcohol−dielectric flat interface.

f, GHz	D, mm	w_{tv0}, J/cm^2	δ, cm	ΔT, K
3	600	0.0402	1.17	0.0365
10	200	0.376	0.707	0.565

2. Numerical simulation

As noted above, CST Microwave Studio program was used for computer simulation of thermal processes. The calculated geometry for modeling absorbing loads with a flat input window is presented above (Fig. 2). The data for calculations were used, including the parameters of the microwave pulse listed in Table 1. Figure 5 shows the

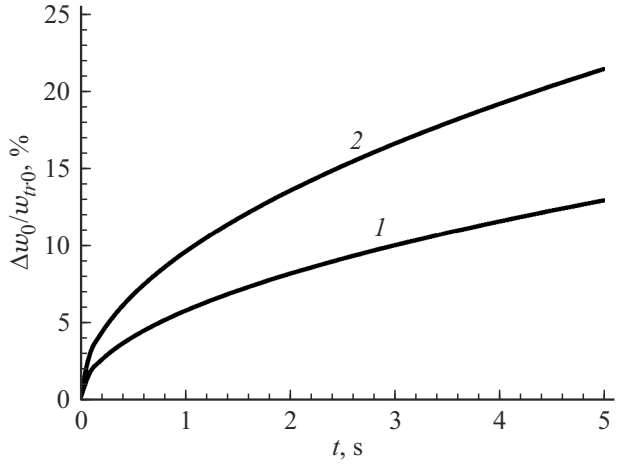

Figure 4. Results of analytical estimates of the time dependence of the relative dissipation of heat from the working fluid to the dielectric for frequencies 3 (*1*) and 10 GHz (*2*).

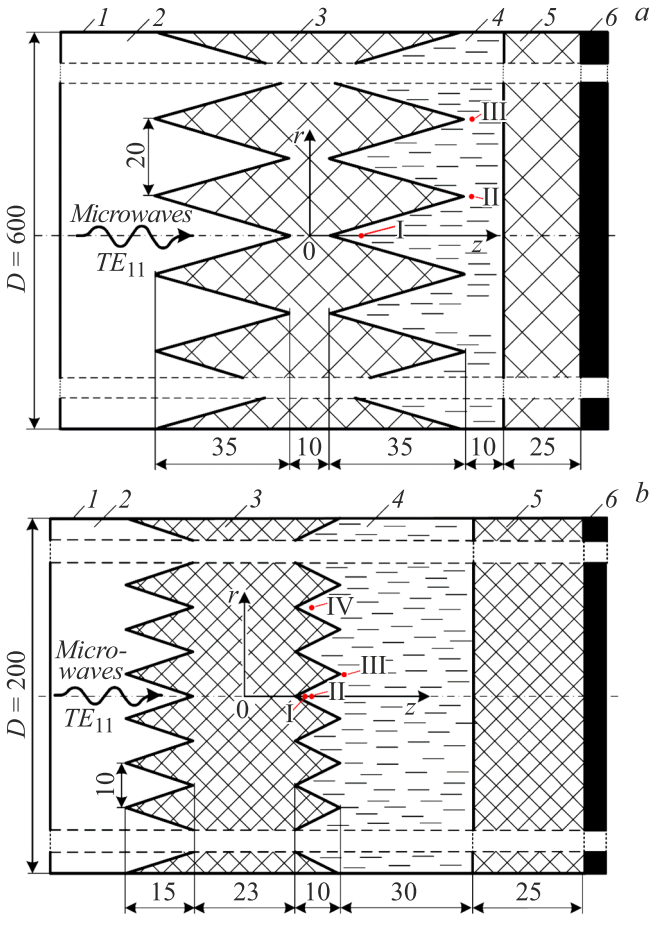

Figure 5. Calculated geometries of absorbing loads for the carrier frequency 3 (*a*) and 10,GHz (*b*): *1* — waveguide; *2* — air; *3* — polyethylene input window; *4* — alcohol; *5* — back wall; *6* — microwave absorber. Roman numerals mark the points where the temperature of the working fluid was calculated after absorption of the microwave pulse. The dimensions are given in millimeters.

calculated geometries of absorbing loads with ribbed input windows for frequencies 3 and 10 GHz. The condition $D \gg \lambda$ is met for both loads, as well as for loads with flat input windows.

A vertically polarized wave TE_{11} incident on each of the four loads was set at frequencies 3 and 10 GHz as in the analytical estimates.

The calculated reflectance of microwave power from the load shown in Fig. 5, *a* ($f = 3$ GHz) is $K_r = -18.7$ dB, microwave power transmitted into alcohol — $P_{tr} = 572$ MW, and microwave energy absorbed in alcohol — $W_{tr} = 57.2$ J. For the load shown in Fig. 5, *b*, ($f = 10$ GHz) $K_r = -23.5$ dB, $P_{tr} = 577$ MW, $W_{tr} = 57.7$ J.

An electrodynamic calculation of the structure of electric and magnetic fields established during the microwave pulse and the distribution of the density of microwave power absorbed in the working fluid was performed for each load. Then, appropriate sources of thermal power were set in the Thermal module (Conjugate Heat Transfer Solver), based on the data of electrodynamic calculations, and computer simulation of thermal processes was performed. The temperature T of the working fluid at various points and its dependence on time was calculated. The calculation of the heat flux from the working fluid into the dielectric material of the input window through its entire surface was performed and the convection flows of the liquid were simulated.

3. Analysis of the results

3.1. Absorbing loads with flat input windows

The requirements for computer simulation conditions, consisting in determining the size of spatial cells and the time step, were determined taking into account the comparison of calculation results and analytical estimates of the temperature distribution of the working fluid along the axis z for loads with flat input windows (Fig. 2).

The initial (immediately after exposure to a microwave pulse) dependence of the temperature of the working fluid calculated with an electrodynamic module on the coordinate z is determined by the corresponding distribution of the absorbed specific microwave energy. The problem is a narrow area near the interface in this case. A temperature jump with a large along z gradient is formed near the interface after exposure to a microwave pulse. This leads to the fact that the maximum $P_T(0)$ of dependence of the heat flux $P_T(t)$ from the working fluid to the dielectric of the input window noticeably changes from time to time in case of a change of the grid size and time step, and the form of dependence $P_T(t)$ changes near $t = 0$. Both stabilize and begin to correspond to the analytical results in the case of a flat window as the cell sizes and the time step decrease. It was necessary to use (and in the case of ribbed windows, too) the cell sizes and the time step, which in fact were determined by the capabilities of the computer's graphics card. Extrapolations of the form $P_T(t) \sim 1/\sqrt{t}$

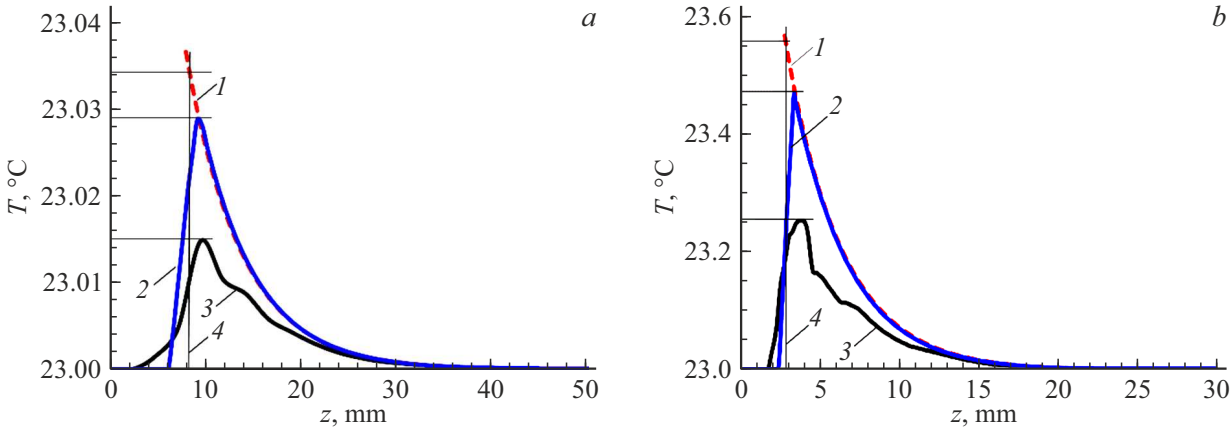

Figure 6. Temperature distribution of the working fluid along the axis z for absorbing loads with a flat input window at a frequency of 3 (a) and 10 GHz (b): *1* — analytical calculations, *2* — calculation results in the electrodynamic module, *3* — calculation results in the Thermal module, *4* — the position of the interface between the dielectric and the liquid.

were introduced, similar to (1) in analytical assessments for additional adjustments of estimates of errors in calculations of heat dissipation near $t = 0$.

The temperature of the working fluid before exposure to the microwave pulse was set to 23°C in the calculations.

Figure 6 shows the temperature distributions of the working fluid along axis z obtained from analytical calculations and simulation.

It can be seen from the graphs that the results of simulation using the electrodynamic module correspond well to the results of analytical calculations. They show (in accordance with the above in sect. 1) an exponential decrease of temperature increment with distance from the interface between the working fluid and the dielectric of the flat input window. At the same time, the difference between these results and the simulation results in the Thermal module is noticeable. It can be assumed that this difference is attributable to the peculiarities of conversion of data of the distribution of the specific absorbed power of microwave radiation of the electrodynamic module into data on the distribution of the specific heat release power of the Thermal module. This, in turn, may be attributable, for example, to a difference in the features of the division of the computational domain in these modules. Unfortunately, it was not possible to find out the reasons for this difference using the description of the CST Microwave Studio program available to the authors.

The results of computer calculations of the time dependencies of heat fluxes $P_T(t)$ and the relative dissipation of heat into the flat input windows of absorbing loads are shown in Fig. 7.

As noted above, a temperature jump occurs immediately after the absorption of the microwave pulse energy in the liquid at the interface with the dielectric, providing a theoretically infinitely large heat flux in accordance with (1), which cannot be precisely determined in numerical calculation because of the finite step in spatial coordinate. This results in some underestimation of the heat ΔW dissipated into the dielectric. This underestimation was evaluated by extrapolation of the results of numerical calculations in the initial short periods of time for all four absorbing loads with dependencies similar to (1) of the form $P(t) \sim 1/t^{0.5}$ so that they smoothly interfaced with the curves obtained as a result of simulation and $\Delta W \sim t^{0.5}$. The data presented in Fig. 7, *a, b,* allowed calculating the relative heat dissipation $\Delta W/W_{tr}$ in flat windows for different time intervals. The results of these calculations are shown in Fig. 7, *c, d*.

It can be seen that the dependencies $P_T(t)$ have a pronounced decline area and noticeably differ from the analytical dependencies shown in Fig. 4. This difference is attributable to the difference of the initial temperature distributions — a step in the case of Fig. 4 and a temperature jump followed by exponential declines in the case of Fig. 7. In the latter case, the decrease of the heat flux into the dielectric can be explained by a more significant decrease in time in the temperature gradient in the working fluid from the side of the input window.

Fig. 8 shows temperature distributions and convection fluxes after exposure to a microwave pulse for both loads.

It can be seen that the highest temperature of the working fluid is observed after 1 s near its interface with the dielectric of the input window. The maximum convection velocity of the working fluid is $\sim 5 \cdot 10^{-4}$ m/s for a frequency load of 3 GHz and $\sim 4 \cdot 10^{-3}$ m/s — for a frequency load of 10 GHz. The corresponding liquid displacements can be 2.5 and 20 mm for time 5 s. Convection of the heated liquid, apart from the top and bottom, occurs mainly along the surface of the windows, which does not contribute to the effective dissipation of heat from the window surfaces. It can be assumed that the convection mechanism does not play a significant role in the processes of change of the spatial distribution of the temperature of the working fluid over time in the case of a load at 3 GH and may have some significance in the case of a load for a frequency of 10 GHz (a somewhat complicated dependence $P_T(t)$, Fig. 7, *b*).

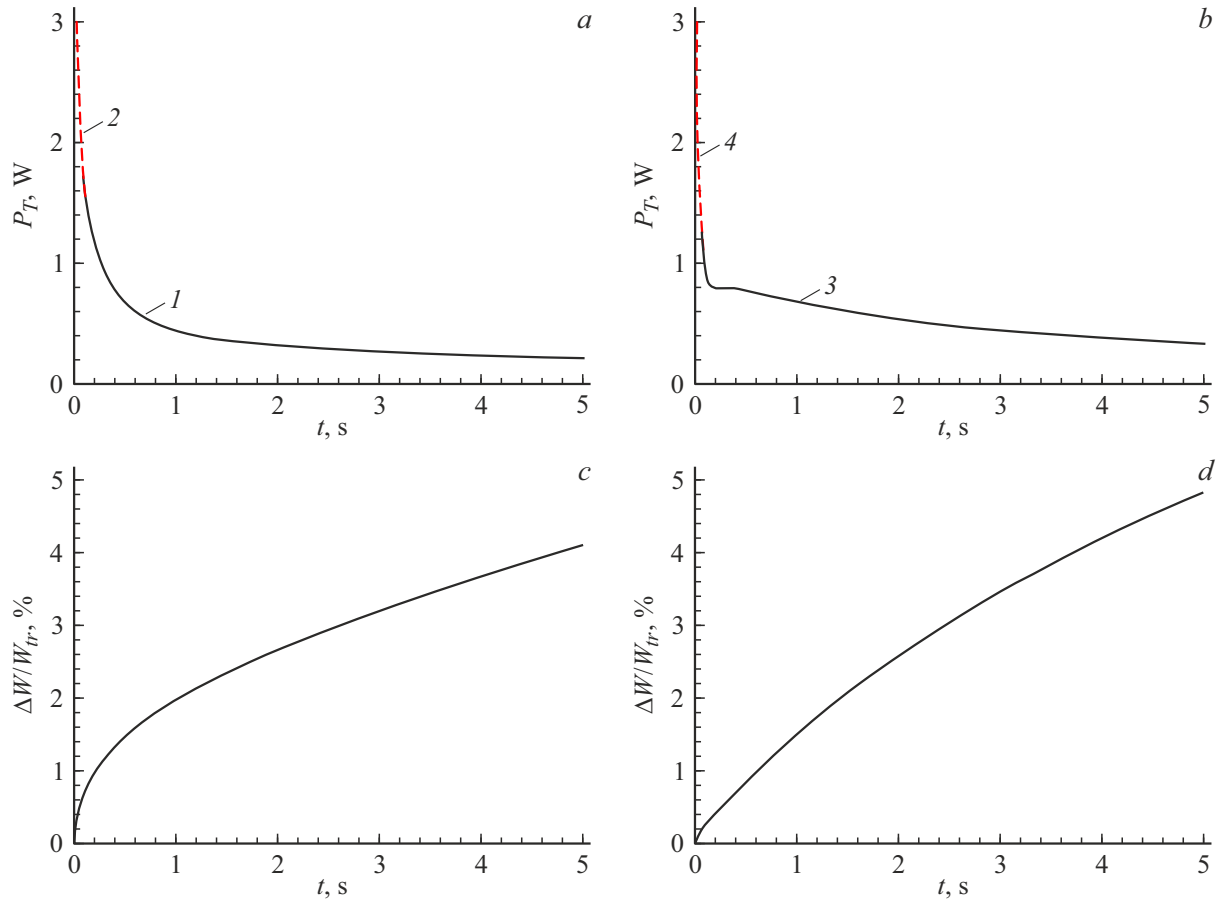

Figure 7. Depending on the time of heat fluxes (a, b) and relative heat dissipation (c, d) from the working fluid to the flat input windows for frequency 3 (a, c) and 10 GHz (b, d): *1* and *3* — computer simulation, *2* — extrapolation using the formula $P_T(t) = 0.5/t^{0.5}$ for $0 \le 0.1111$ s, *4* — extrapolation using the formula $P_T(t) = 0.33/t^{0.5}$ for $0 < t \le 0.0861$ s.

Estimates and computer simulations (Figs. 4 and 7) show that thermal losses for a frequency of 10 GHz exceed losses for a frequency of 3 GHz, which may be explained by a higher initial difference ΔT at the interface of the working fluid and the dielectric in the case of a frequency of 10 GHz. Taking into account the extrapolated dependencies provides an increase of losses by no more than 8% for an absorbing load at a frequency of 3 GHz and no more than 0.2%for a load at a frequency of 10 GHz.

The relative heat dissipation into flat windows obtained as a result of computer simulation do not exceed 5% and are significantly less than in analytical estimates. Computer simulation more fully accounts for heat transfer processes and therefore provides more accurate results. Estimates for flat windows based on the half-space cooling model may have limited application during the first seconds immediately after absorption of microwave energy and are quite rough, providing an overestimated heat loss.

3.2. Absorbing loads with ribbed input windows

In absorbing loads with ribbed input windows, compared with loads with flat windows, the structure of the electromagnetic field and the density distribution of absorbed microwave energy are complicated by the ribbed surface of the dielectric. The ribbed surface of the window also affects the process of convection of the working fluid.

Fig. 9, *a, b* presents the results of computer calculations of time dependencies of heat fluxes $P_T(t)$ in the ribbed input windows of absorbing loads. Extrapolations $P(t) \sim 1/t^{0.5}$ and $\Delta W \sim t^{0.5}$ were used to clarify the heat fluxes in small initial time intervals like in the case of flat windows. Relative heat dissipation into the ribbed input windows $\Delta W/W$ (Fig. 9, *c, d*) calculated based on the data presented in Fig. 9, *a, b*. A sharper relative decrease in heat fluxes over a period of about 1 s is noticeable in contrast to the case of flat windows. Moreover, prolonged (not less than 15 s) weak return heat fluxes from heated dielectric surfaces into the working fluid begin after 1.7 s for a load of 3 GHz and after 0.5 s for a load of 10 GHz which can be associated with convection which is capable of removing heat from the surface of the ribs unlike the case of flat windows, although the convection has low velocities.

The relative heat loss reaches 11.5% for 3 GHz load and 13% for 10 GHz load taking into account extrapolations.

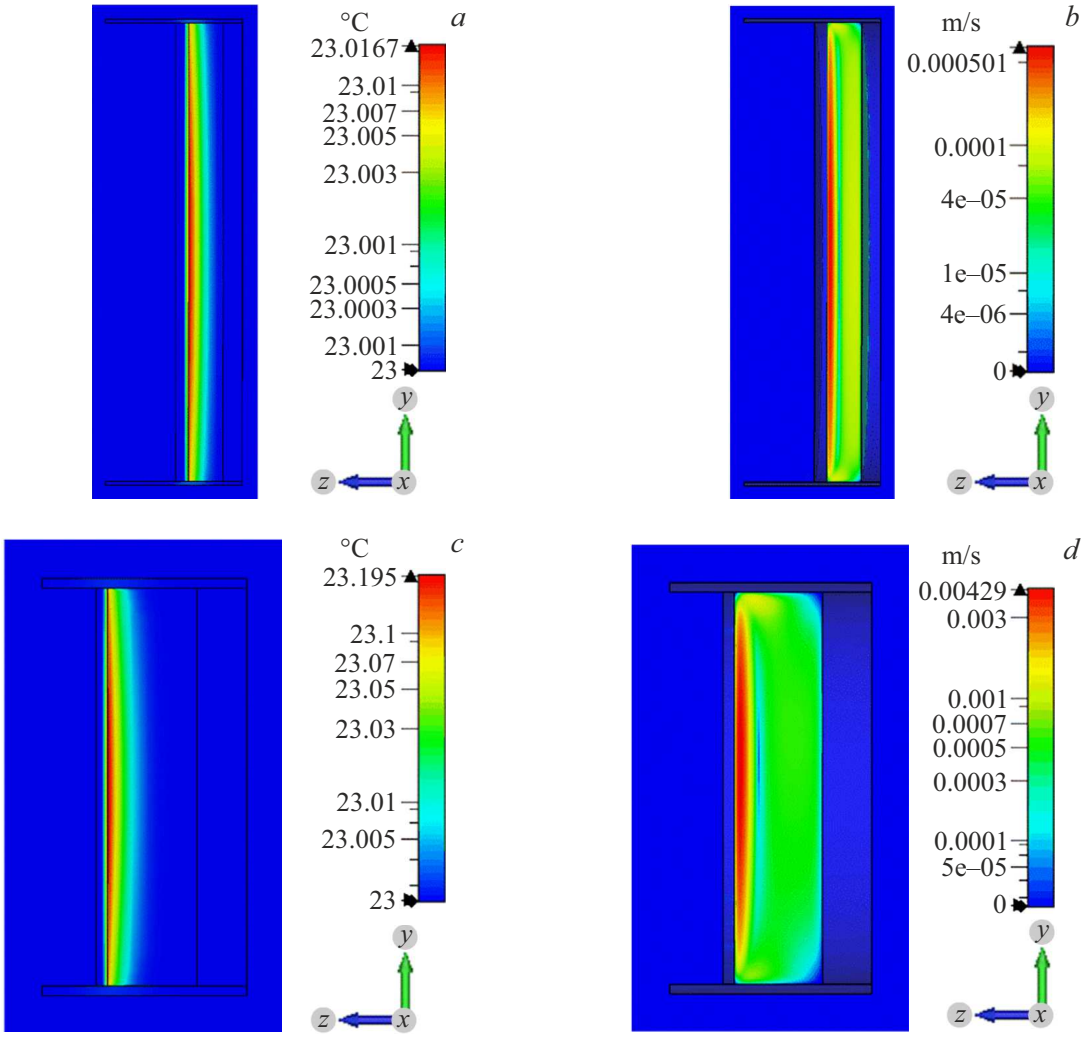

Figure 8. Temperature distributions (a, c) in 1 s and convection fluxes (b, d) in 5 s after exposure to a microwave pulse for absorbing loads at 3 (a, b) and 10 GHz (c, d) with flat input windows.

These values are more than 2 times higher than the relative heat loss in the case of flat windows. Such a difference, apparently, can be attributable to the fact that the contact surface of the working fluid and the dielectric in the case of ribbed windows is larger than in the case of flat windows. In addition, it is necessary to take into account described below features of the temperature distribution of the working fluid near the surfaces of the ribbed input windows, which is more complex than in the case of flat input windows.

The relative heat loss for both loads increases by about 22% compared to purely computer modeling if the extrapolated dependencies are taken into account.

Unfortunately, it can be assumed that the calculated values of heat dissipation into the dielectric of the input window are somewhat underestimated compared to the actual values due to the above-mentioned features of the Thermal module, like in the case of flat windows.

Fig. 10 shows the temperature distribution and convection fluxes after exposure to a microwave pulse for both absorbing loads with ribbed input windows.

It can be seen that the microwave energy is released near the dielectric surface of the ribs. The maximum convection velocity of the working fluid is less than in the case of flat windows and is $\sim 2 \cdot 10^{-4}$ m/s for a 3 GHz frequency load and it amounts to $\sim 7 \cdot 10^{-4}$ m/s for a 10 GHz frequency load. The corresponding liquid displacements can be as low as 1 and 3.5 mm during the time of 5 s. Therefore, it can be assumed that the convection of the working fluid in the case of ribbed windows has a weak effect on heat transfer processes.

Table 3 provides the increments ΔT of the working fluid temperature in loads with ribbed input windows at some points of the working fluid immediately after exposure to a microwave pulse. The largest increment of the working fluid temperature, as follows from the data in Table 3, is in the grooves of the ribs, which is apparently associated with

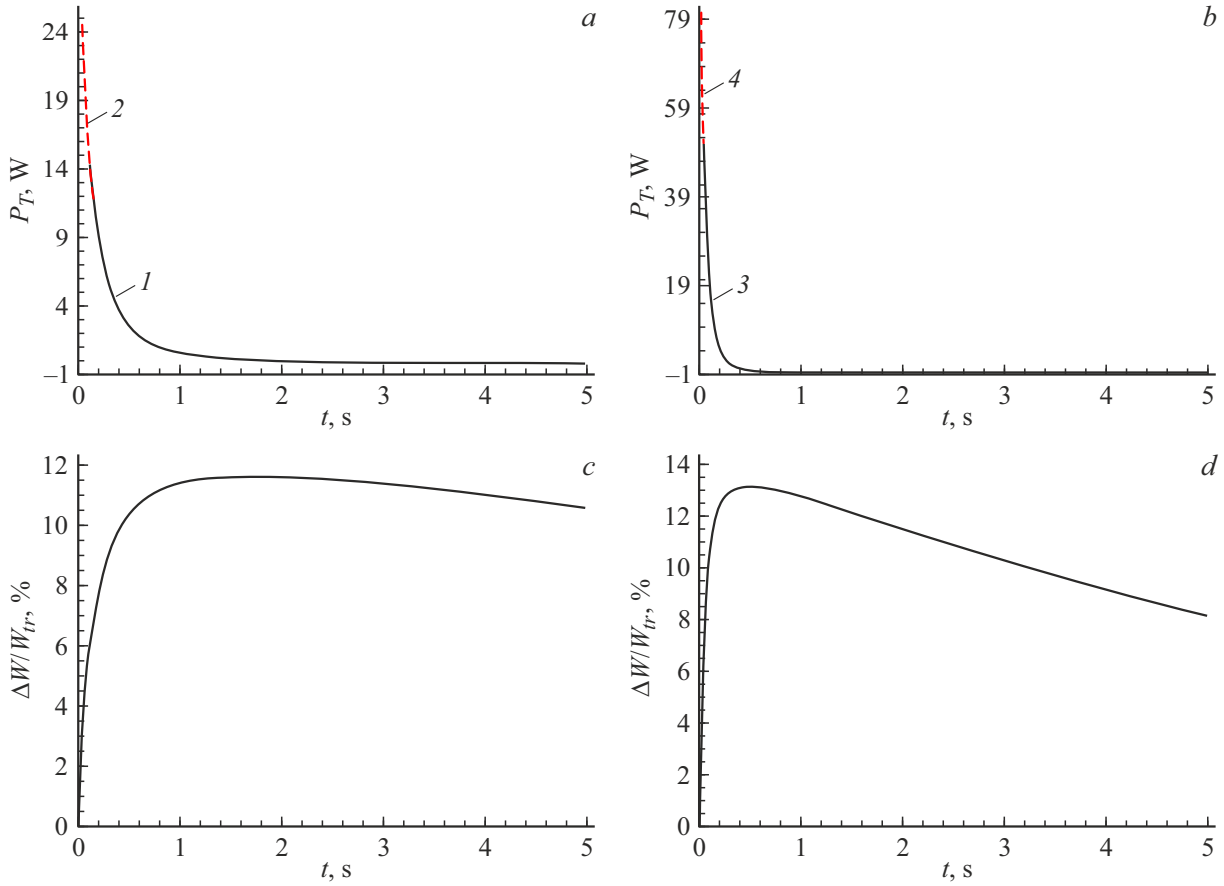

Figure 9. Depending on the time of heat fluxes (a, b) and relative heat dissipation (c, d) from the working fluid to the ribbed input windows for frequency 3 (a, c) and 10 GHz (b, d): *1* and *3* — computer simulation, *2* — extrapolation by the formula $P_T(t) = 4.5/t^{0.5}$ for $0 < t < 0.1278$ s, *4* — extrapolation by the formula $P_T(t) = 10.38/t^{0.5}$ for $0 < t \leq 0.04$ s.

Table 3. Temperature increments at various points of the absorbing loads shown in Fig. 5

	Fig. 5, *a*, 3 GHz			Fig. 5, *b*, 10 GHz			
№	I	II	III	I	II	III	IV
r, mm	0	10	30	0	0	5	20
z, mm	13	41	41	13.5	15	23	15
ΔT, K	0.0102	0.00104	0.00478	1.84	0.374	0.0553	0.178

the higher electric field strength as a result of interference. Such locally increased increments ΔT of the working fluid temperature near the surfaces of the ribbed input windows can yield a higher relative heat dissipation into the dielectric compared to flat windows.

Conclusion

The performed studies have shown satisfactory agreement of distributions of the specific absorbed microwave energy and the increments of the working fluid temperature, obtained in analytical estimates and electrodynamic calculations of the CST Microwave Studio package for flat input windows. The calculated temperature increments with a maximum at the interface between the working fluid and the dielectric of the input window, related to the density of the microwave power flux, are of practical importance for determining the maximum microwave energy that can be applied to the absorbing load of the calorimeter. Bubbles can be formed and the performance of the calorimeter can significantly deteriorate, up to its complete loss, if the working fluid temperature exceeds a critical value. The result associated with data on locations with the highest temperature increase and its magnitude has a similar significance in the case of ribbed input windows.

The nature of heat transfer between the working fluid and the dielectric of the input window, along with the initial distribution of absorbed energy and thermal conductivity, can be influenced by convection.

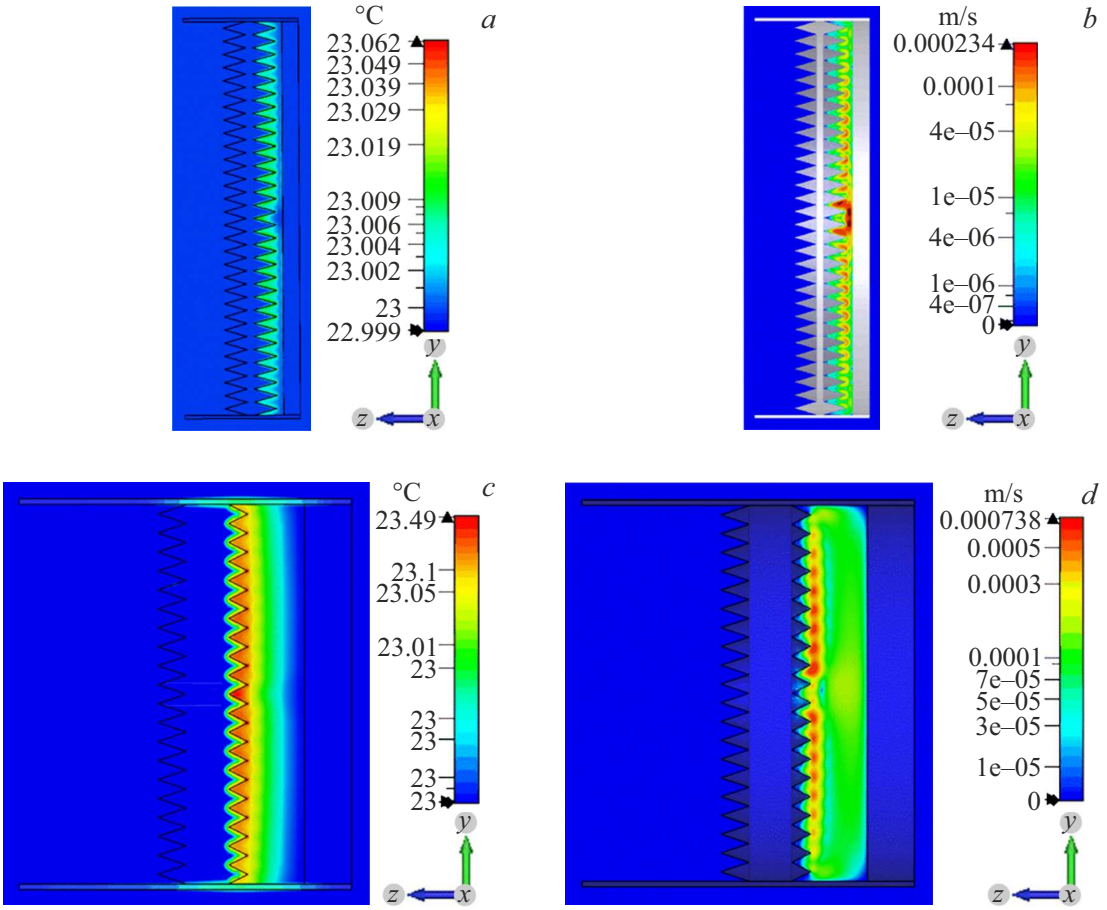

Figure 10. Temperature distribution in 1 s (a, c) and convection fluxes (b, d) in 5 s after exposure to a microwave pulse for absorbing loads at 3 (a, b) and 10 GHz (c, d) with ribbed input windows.

The characteristic times of the heat transfer processes are within a few seconds, which corresponds to the typical time of the mechanical reaction of the absorbing load and the response time of the measuring system of the calorimeter.

The relative dissipation of heat into the dielectric material of the ribbed windows of wide-aperture disk-shaped absorbing loads of calorimeters with an ethyl alcohol-based working fluid, characterizing a systematic underestimation of the measured energy of a high-power microwave pulse, can be comparable with the typical error of the calorimeter $\pm(10-20)\%$, mainly due to environmental impact.

Funding

The study has been performed under the state assignment of the Ministry of Science and Higher Education of the Russian Federation (topic № FWRM-2021-0002).

Conflict of interest

The authors declare that they have no conflict of interest.

References

[1] A.I. Klimov. Rus. Phys. J., **62** (7), 1260 (2019). DOI: 10.1007/s11182-019-01843-4

[2] A.I. Klimov, V.Yu. Konev. *Proc. 8th Int. Cong. Energy Fluxes Rad. Effects* (Tomsk, Russia, 2022), p. 275. DOI: 10.56761/EFRE2022.S3-P-016807

[3] A.G. Shkvarunets. Instr. Exp. Tech., **39** (4), 535 (1996).

[4] D.V. Sivukhin. *Kurs obshchej fiziki. T. 2. Termodinamika i molekulyarnaya fizika* (Fizmatlit, M., 2005) (in Russian).

[5] *Engineering ToolBox. The density of ethyl alcohol vs temperature* [online]; https://www.engineeringtoolbox.com/ethanol-ethyl-alcohol-density-specific-weight-temperature-pressure-d_2028.html

[6] *Engineering ToolBox. Heat capacity of ethyl alcohol as a function of temperature* [online]; https://www.engineeringtoolbox.com/specific-heat-capacity-ethanol-Cp-Cv-isobaric-isochoric-ethyl-alcohol-d_2030.html

[7] *Engineering reference book. Tables DPVA.ru. Ethyl alcohol, ethanol — properties.* [online]; https://dpva.ru/Guide/GuideMedias/Spirits/EtanolPrperties1999/

[8] L.D. Landau, E.M. Lifshits. *Elektrodinamika sploshnykh sred* (Nauka, M., 2005) (in Russian)

[9] J.-Z. Bao, M.L. Swicord, C.C. Davis. J. Chem. Phys., **104** (12), 4441 (1996). DOI: 10.1063/1.471197
[10] I.V. Lebedev. *Tekhnika i pribory SVCH* (Vysshaya shkola, M., 1970), t. 1. (in Russian).
[11] A.L. Feldshtein, L.R. Yavich, V.P. Smirnov. *Spravochnik po elementam volnovodnoj tekhniki* (Sov. radio, M., 1967) (in Russian).

Translated by A.Akhtyamov